PERGAMON
Vision Research 41 (2001) 3215–3228
Research
www.elsevier.com/locate/visres

Direction of heading and vestibular control of binocular eye movements

Dora E. Angelaki [a,*], Bernhard J.M. Hess [b]

[a] *Department of Anatomy and Neurobiology, Box 8108, Washington University School of Medicine, 660 South Euclid Avenue, St Louis, MO 63110, USA*
[b] *Department of Neurology, University Hospital Zurich, Zurich, Switzerland*

Received 5 September 2000; received in revised form 15 November 2000

Abstract

To optimize visual fixation on near targets against translational disturbances, the eyes must move in compliance with geometrical constraints that are related to the distance as well as the speed and direction relative to the target. It is often assumed that the oculomotor system uses the vestibular signals during such movements mainly to stabilize the foveal image irrespective of the peripheral vision. To test this hypothesis, trained rhesus monkeys were asked to maintain fixation on isovergence targets at different horizontal eccentricities during 10 Hz oscillations along different horizontal directions. We found that the two eyes moved in compliance with the geometrical constraints of the gaze-stabilization hypothesis, although response gains were generally small (~ 0.5). The best agreement with the gaze stabilization hypothesis occurred for heading directions within $\pm 30°$ from straight-ahead, whereas lateral movements exhibited greater variability and larger directional errors that reflected the statistical response variability inherent in the non-linear dependence on heading direction. In contrast to undercompensatory version (conjugate) components, the disjunctive part of the response (vergence) exhibited unity or higher than unity gains. The high vergence gains might reflect a strategy that aims at maintaining the binocular coordination of the gaze lines despite the low gain of the version movements. © 2001 Elsevier Science Ltd. All rights reserved.

Keywords: Oculomotor; Monkey; Hypothesis; Binocular; Vergence; Version; Gaze stabilization; Foveal vision

1. Introduction

Linear disturbances of the head result in distortions of the visual field that depend critically on the relative directions of motion and gaze. When the two are nearly parallel these distortions can be described as radial expansions of the retinal image that cannot be compensated by a single eye movement. Since visual acuity strongly degrades from the fovea towards the retinal periphery, a way out of this dilemma could be a strategy that minimizes image slip on the fovea at the expense of stability of the peripheral retinal image. As foveal vision emerged together with stereovision, novel visual and vestibular mechanisms have evolved to help stabilizing binocular gaze on targets during linear disturbances of the head (Miles, Schwarz, & Busettini, 1991; Miles, 1998). Primates, for example, have developed highly specialized vestibular mechanisms that are capable of eliciting robust short-latency (< 10 ms) eye movements, known as translational vestibulo-ocular reflexes (trVOR), in response to linear head displacements (Schwarz, Busettini, & Miles, 1989 Paige & Tomko, 1991a Paige & Tomko, 1991b Schwarz & Miles, 1991 Bush & Miles, 1996 Telford, Seidman, & Paige, 1997 Angelaki & McHenry, 1999). These reflexes operate in concert with short-latency low-level visual mechanisms to optimize binocular gaze stability during linear disturbances (Busettini, Miles, & Schwarz, 1991 Busettini, Miles, Schwarz, & Carl, 1994 Busettini, Masson, & Miles, 1996a Busettini, Miles, & Krauzlis, 1996b Busettini, Masson, & Miles, 1997 Masson, Busettini, & Miles, 1997).

During translation, otolith afferents simply encode the direction of head movement, without an a priori relation to gaze parameters. In fact, depending on the functional requirements, the oculomotor system could

* Corresponding author. Tel.: +1-314-7475529; fax: +1-314-7475069.
E-mail address: angelaki@thalamus.wustl.edu (D.E. Angelaki).

PII: S0042-6989(00)00304-7

take advantage of these signals to stabilize selective parts of the visual field by generating the appropriate eye movement. Along these lines, it has been assumed that the trVORs are tuned to stabilize images on the fovea (Paige & Tomko, 1991a,b; Tomko & Paige, 1992). According to this hypothesis, these reflexes should exhibit a precise dependence on eye-to-target distance and relative eye-to-target motion. Tomko & Paige (1992) have reported that the sensitivity of each eye to head translation follows qualitatively the expected dependence on eye position for heading directions in the range of $\pm 30°$ from straight-ahead. Nevertheless, a thorough test of the validity of the gaze stabilization hypothesis is still missing and the binocular aspects have not yet been addressed. It is not known, for example, how well the movement of each eye is controlled by target location and heading direction. Moreover, the proposed gaze-stabilization hypothesis has been based on a cyclopean representation. However, the fact that trVOR gains are low for large vergence angles (Paige & Tomko, 1991a,b; Schwarz & Miles, 1991; Telford et al., 1997; Angelaki, McHenry, & Hess, 2000a; Angelaki, McHenry, Dickman, & Perachio, 2000b; McHenry & Angelaki, 2000) raises questions about the role of trVOR in binocular coordination and stereovision. In the present study, we have addressed this issue by examining binocular gaze velocity as a function of eye-to-target distance and relative eye-to-target motion during high frequency oscillations on a linear sled. Using a binocular model that has been derived based on the ideal geometry of binocular fixation, we quantitatively tested the gaze stabilization hypothesis and its sequelae on binocular gaze control.

2. Methods

2.1. Animal preparation and training

Data presented here were obtained from four juvenile rhesus monkeys that were implanted with a lightweight delrin head ring and dual eye coils on each eye, as described in detail elsewhere (Angelaki, 1998; Angelaki et al., 2000a). All animals were trained with juice rewards to fixate randomly presented red LED targets. Adequate fixation was determined online by comparing binocular horizontal and vertical eye positions with ideal target position windows of $\pm 1°$. Animals were usually trained 5 days/week with free access to water on the weekend. All animal surgeries and experimentation were in accordance to Institutional and NIH guidelines.

2.2. Experimental set-up and protocols

During vestibular testing, animals were rigidly secured to the inner axis of a three-dimensional rotator mounted on a linear sled (Acutronics, USA). Animals were secured with lap and shoulder belts to a primate chair and their limbs were loosely bound. In all experiments, the head was statically pitched 18° nose-down from the horizontal stereotaxic plane. Special care was taken to rigidly couple the animal's head to the fiberglass inner gimbal of the motion delivery system and a head coil was used to ascertain that there was no head movement signal during the motion (for details, see Angelaki, 1998; Angelaki et al., 2000a). The linear acceleration stimuli consisted of 10 Hz sinusoidal oscillations (peak acceleration 0.32 g, peak velocity 5.1 cm/s). Onset of motion was contingent upon adequate fixation (300–1000 ms) of a randomly selected head-fixed LED target (see below). Binocular eye positions were computed on-line to monitor fixation based on geometrical target position windows as described elsewhere (Angelaki et al., 2000a).

During translation, perfect racking of a stationary target in the horizontal plane depends on three factors: current right and left eye position (θ_R and θ_L), heading direction (α), and vergence angle (ε; related to target distance (see Appendix A; also Paige & Tomko, 1991b; Telford et al., 1997; McHenry & Angelaki, 2000). In order to study response sensitivity as a function of gaze and heading direction, it was advantageous to present fixation targets that subtend the same vergence angle. These targets were positioned every 2.5° on a horizontal isovergence screen (8.6°) subtending a total visual angle of 40° (cf., McHenry & Angelaki, 2000).

Demodulated eye coil signals (four for each eye) and the outputs of a three-axis accelerometer (rigidly attached to the fiberglass members to which the magnetic field coil assembly and the animal's head were firmly attached) were anti-alias filtered (200 Hz, six-pole low pass Bessel). The signals were digitized at 833.3 Hz (Cambridge Electronics Design, model 1401 plus, 16-bit resolution) and stored for off-line analysis.

2.3. Data analyses

Eye movements were calibrated using a combination of pre-implantation and daily calibration procedures, as previously described (Angelaki, 1998; Angelaki et al., 2000a; Angelaki et al., 2000b). Binocular, three-dimensional eye position was computed as rotation vectors (Haustein, 1989) with straight ahead as the reference position. The signals were smoothed and digitally filtered as described elsewhere (Angelaki et al., 2000a). Eye angular velocity (Ω) was subsequently computed and used for the remaining analyses. Torsional, vertical and horizontal eye movements were defined as the components along the x- (fore–aft), y- (interaural) and z- (vertical) head axes (positive axis directions are forward, leftward and upward, respectively).

Average response cycles from a manually selected saccade-free steady-state portion (i.e. starting a mini-

mum of three cycles after motion onset) from each experimental trial were computed for the three components of each eye velocity, the horizontal vergence velocity $\dot{\varepsilon} = \dot{\theta}_R - \dot{\theta}_L$, the horizontal version velocity $\dot{\sigma} = (\dot{\theta}_R + \dot{\theta}_L)/2$, as well as the stimulus (vectorial sum of the two outputs of a 3-D linear accelerometer mounted close to the animal's head). A sinusoidal function including first and second harmonics and a DC offset were fit to each average cycle with a non-linear least squares optimization algorithm based on the Levenberg–Marquardt method (MATLAB, Mathworks, Inc.). For each eye velocity component, as well as vergence and version, sensitivity was then computed as the ratio of the respective peak sinusoidal amplitude to peak linear head velocity (in °/s per cm/s, which is equivalent to °/cm). Peak linear head velocity was computed from the linear acceleration fits. Response phase was expressed as the difference between each eye (or vergence and version) velocity relative to linear head velocity. Positive linear acceleration is defined to be rightward and forward for the y- and x-components of the linear accelerometer output, respectively. Because leftward eye movements are defined here to be positive, a phase of 0° corresponds to a compensatory response during lateral motion. Similarly, during fore–aft motion, compensatory phase should be 0° when looking to the left and 180° when looking to the right. The sensitivity and phase estimates, as well as mean eye position over the first stimulus cycle, were stored for each experimental run. The second harmonic component fit was generally at least an order of magnitude less than the fundamental component and was not considered further.

2.4. Model simulations and model fits

To evaluate quantitatively the dependence on gaze and heading directions, we derived equations describing the movement of each eye under the assumption that the animals track the target perfectly during the entire phase of the head movement (see Appendix A). The velocity sensitivity of the VOR in the horizontal plane was found to be proportional to the respective eye–target distance and the sine of the difference between the angles that gaze and heading direction subtended relative to straight ahead (Eq. (A2)). This equation can be re-expressed as a function of vergence angle and interocular distance (Eqs. (A5a) and (A5b), as well as Eqs. (A8) and (A9) for version and vergence). Whereas the eye–target distance differed for each fixation target, vergence angle was constant for all targets on the isovergence screen.

To quantify the gaze stabilization model, Eqs. (A5a), (A5b), (A8) and (A9) were fitted (non-linear least-squares method) to the right and left eye movement data, as well as to version and vergence eye movements, in one of three ways. First, data for all gaze directions were fitted separately for each heading direction. Second, data for all heading directions were fitted separately for each of five gaze directions by pooling the data in bins of $\pm 2.5°$ around the directions $\sigma = -20,\ -10,\ 0,\ 10$ and 20°. Third, the same equations were also fitted to the whole data set from each animal, i.e. to all gaze and heading directions simultaneously. In all three cases, the fitted functions were optimized by allowing two parameters to vary, a 'gain' factor, k, and a directional error, $\Delta\alpha$ (that allowed a shift of the curves to the left or to the right). Ideally, $k = 1$ and $\Delta\alpha = 0$. The goodness of fit was evaluated by computing the mean-square-error. Statistical comparisons were based on analyses of variance with two factors, animal and heading or gaze direction. Specifically, the k and the absolute values of $\Delta\alpha$ were investigated for significant differences as a function of gaze and heading directions. The statistical comparisons were based on $n = 7$ levels of heading angles (corresponding to $|\alpha| = 0,\ 15,\ 30,\ 45,\ 60,\ 75$ and 90° away from fore–aft) and $n = 3$ levels of gaze eccentricity (corresponding to $|\sigma| = 0,\ 10$ and 20°).

3. Results

3.1. Simulations of compensatory responses

If the eye movements elicited during high frequency oscillations in different directions complied with the kinematic model, Eqs. (A5a) and (A5b) would describe the dependence of the trVOR on heading direction. This ideal response behavior has been plotted as a function of the respective gaze eccentricity in Fig. 1 (red and blue lines for the right and left eye, respectively). During fore–aft motion ($\alpha = 0°$), the response sensitivity is zero for straight-ahead gaze ($\theta = 0°$) and increases with eccentric eye position. As the heading direction moves away from the fore–aft axis, the tuning curves shift in the respective direction such that the zero-sensitivity point corresponds to gaze directions that are aligned with the axis of head translation (i.e. displaced from straight-ahead through angle α). For example, during translation along a direction $\alpha = +15°$ (i.e. the animal is rotated 15° clockwise relative to the axis of sled movement), the response sensitivity of the eye should be zero for a gaze direction of 15° to the left. Similarly, during translation along a direction $\alpha = -15°$ (i.e. the animal is rotated 15° counterclockwise relative to the axis of sled movement), the response sensitivity should be zero for a gaze direction 15° to the right. As the heading direction shifts more and more away from

the fore–aft axis ($>30°$), the slope of the sensitivity curves as a function of eye position becomes shallower whereas the zero sensitivity moves outside the range of gaze directions of $\pm 25°$ (Fig. 1). During lateral motion ($\alpha = \pm 90°$), the right and left eye sensitivities depend minimally on eye position.

The movement of the two eyes should not always be conjugate. Specifically for fore–aft motion ($\alpha = 0°$), vergence sensitivity (defined as the difference between the sensitivities of each eye) should follow a quadratic dependence on eye position that peaks at $\sigma = 0°$ (Eq. (A8); see also Paige & Tomko, 1991b; McHenry & Angelaki, 2000). During lateral motion ($\alpha = \pm 90°$), vergence sensitivity should be zero at $\sigma = 0°$ but increase with increasing eye eccentricity (Fig. 1, green lines). The version component of the response exhibits qualitatively the same dependence as the right and left eye sensitivities (not plotted in Fig. 1).

In the following, we investigate how precisely the vestibularly-driven eye movements during translation comply with the geometrical requirements of the hypothesis that the sensorimotor transformations are optimized for foveal vision.

3.2. Tuning of right and left eye sensitivity

The eye movements elicited during high frequency translation were qualitatively consistent with the tuning predicted based on the gaze-stabilization hypothesis. Examples of the gaze and heading direction dependence of the sensitivity and phase of the movement of the right eye have been illustrated in Fig. 2. During fore–aft motion ($\alpha = 0°$), for example, horizontal response sensitivity increased with eccentric eye position and was zero during fixation at central targets. The phase of the response also shifted 180° for positive and negative eye positions. The 'V-shape' curve of horizontal sensitivity, as well as the phase reversal shifted to the left or to the right along the eye position axis as the heading direction changed away from the fore–aft axis. The further away was heading direction from the fore–aft axis, the smaller the dependence on eye position.

The accuracy with which this dependence approached the theoretical behavior was quantified by fitting Eqs. (A5a) and (A5b) to the whole data set for each animal (thin lines in Fig. 2; fitted parameters are included in Table 1). With the exception of one animal

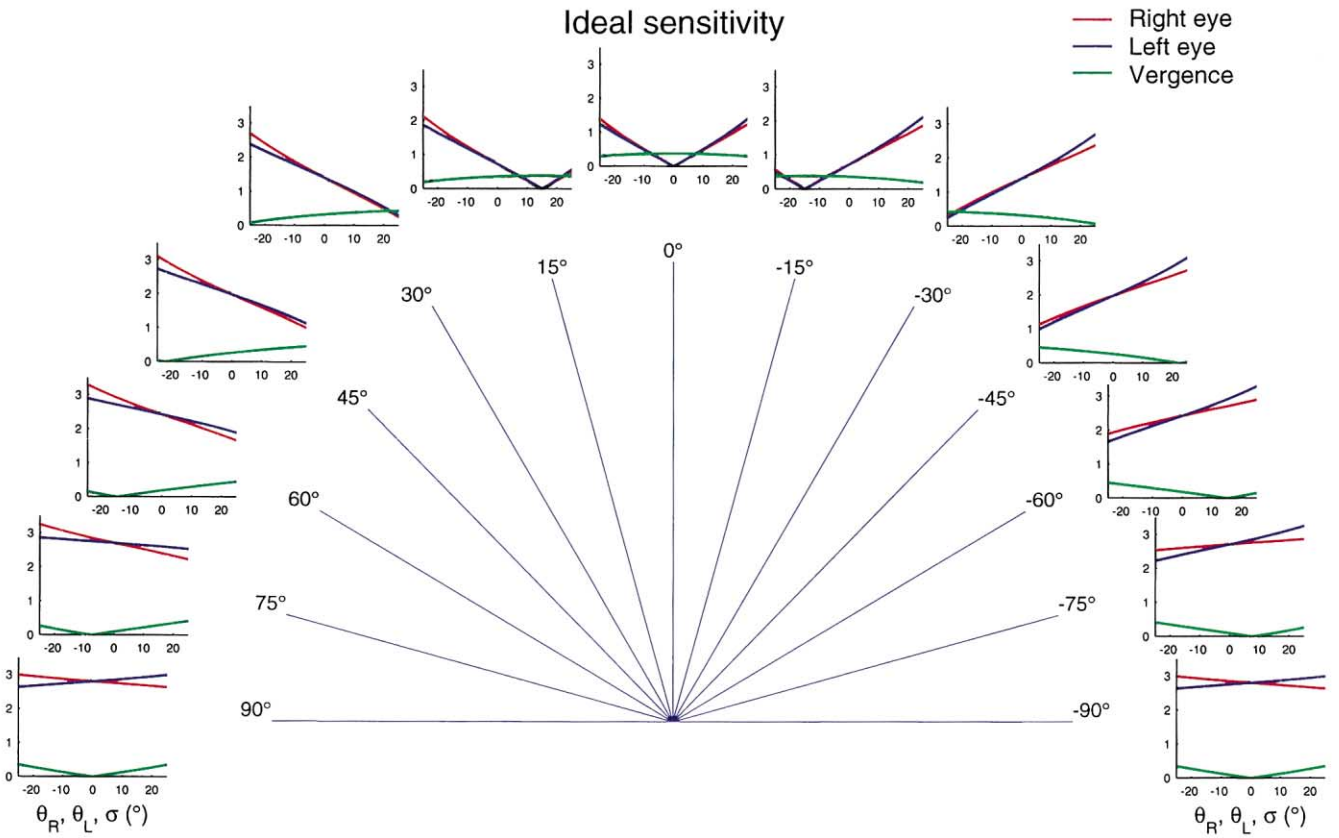

Fig. 1. Geometrical dependence of horizontal eye velocity sensitivity for different heading directions. The ideal horizontal sensitivity (in units of °/cm) of the right eye, the left eye and vergence have been plotted as a function of the respective horizontal eye position (i.e. θ_R, θ_L and σ; red, blue and green lines, respectively). An orientation of $\alpha = 0°$ corresponds to fore–aft motion, whereas orientations of $\alpha = \pm 90°$ correspond to lateral motion stimuli. Simulation parameters: $\varepsilon = 8.6°$ and $d_{ioc} = 3$ cm.

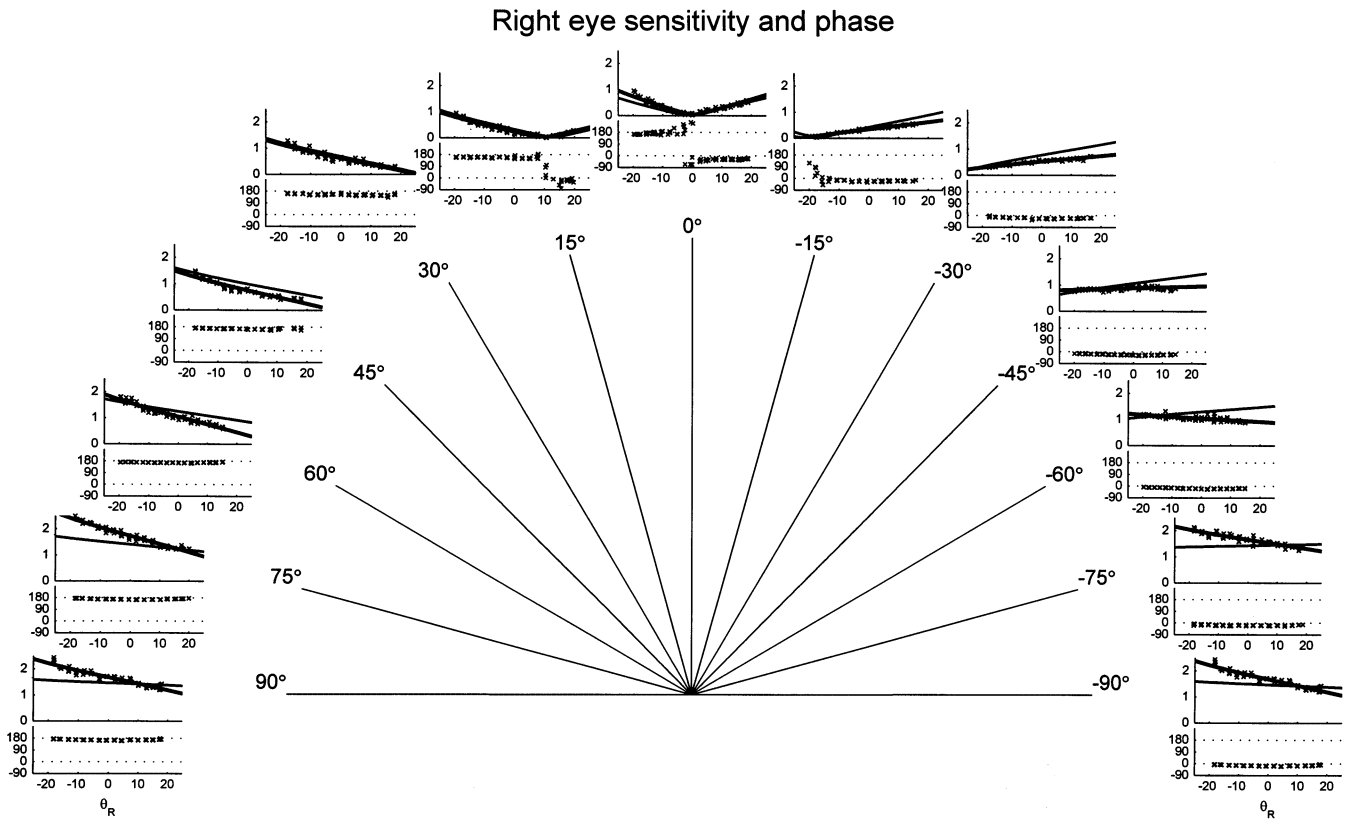

Fig. 2. Tuning of the right eye sensitivity as a function of right eye position (θ_R). Response sensitivity (°/cm) and phase (°) are both plotted for each heading direction. The superimposed thin lines are fits of Eqs. (A5a) and (A5b) to the whole data set (i.e. all heading directions simultaneously; parameters are included in Table 1). The superimposed thick lines are fits of Eqs. (A5a) and (A5b) separately to data for each heading direction. An orientation of $\alpha = 0°$ corresponds to fore–aft motion, whereas orientations of $\alpha = \pm 90°$ correspond to lateral motion stimuli.

Table 1
Global fit parameters for directional error ($\Delta\alpha$) and gain (k)

Animal	Right eye		Left eye		Version		Vergence	
	$\Delta\alpha_R$ (°)	k_R	$\Delta\alpha_L$ (°)	k_L	$\Delta\alpha_s$ (°)	k_s	$\Delta\alpha_\varepsilon$ (°)	k_ε
Animal C	6.0	0.51	11.5	0.52	7.4	0.51	25.5	1.02
Animal D	−2.1	0.52	6.3	0.61	2.6	0.54	−31.8	1.35
Animal G	−2.8	0.52	2.8	0.55	0.3	0.52	9.6	1.13
Animal P	3.4	0.41	0.7	0.35	1.9	0.38	48.5	0.63

(animal C), directional errors estimated from right and left eye responses were small, suggesting that they were appropriately tuned to both heading and gaze directions. Gains, however, were consistently small, averaging ~ 0.5 (Table 1).

In addition to the global fits, the same equations were also fitted to specific data sets in order to evaluate separately the dependence of the trVOR sensitivity on gaze and heading directions. Specifically, Eqs. (A5a) and (A5b) were fitted to the data separately for each heading direction (thick lines in Fig. 2). Results were very similar to those obtained from the global fits. The correlations between the heading directions estimated from these fits (parameters $\alpha + \Delta\alpha_R$ and $\alpha + \Delta\alpha_L$) and the actual heading direction were linear and exhibited a nearly unity slope (Table 2; animal C had the largest deviations from the ideal behavior).

Despite qualitative agreement with the model, however, the fitted parameters departed from the expected ideal values in two respects. First, the estimated gains, k_R and k_L, were always less than unity (Fig. 3). Second, the directional errors between the gaze of the right or left eye and target velocity, $\Delta\alpha_R$ and $\Delta\alpha_L$, depended on heading direction (Fig. 3; for statistical comparisons,

see Table 3). Directional errors were small ($<10°$) for heading directions within $\pm 30°$ of the fore–aft direction. However, errors progressively increased for larger heading angles and became as large as $\pm 40°$ for directions within $\pm 30°$ of the lateral translation.

In addition to fitting data for all gaze directions separately for each heading direction, the following complementary analysis was undertaken. Eqs. (A5a) and (A5b) were also fitted for all heading directions separately after pooling the eye positions in bins of $\pm 2.5°$ around the directions $\sigma = -20,\ -10,\ 0,\ 10$ and $20°$. Examples of such fits are displayed in Fig. 4. As expected from the geometrical model, the VOR sensitivity of the right and left eye exhibited a sinusoidal dependence on heading direction, with a zero-crossing that shifted systematically as a function of gaze orientation. In contrast to the dependence on heading direction, neither directional error $\Delta\alpha$ nor the gain k depended on gaze eccentricity (Table 3).

Table 2
Estimated heading direction ($\alpha+\Delta\alpha$) as a function of stimulus direction (α): linear regression parameters

	Right eye	Left eye
Animal C	$Y=1.10x+8.6$; $r^2=0.98$	$Y=1.26x+23.3$; $r^2=0.97$
Animal D	$Y=1.0x-12.6$; $r^2=0.97$	$Y=1.07x+13.0$; $r^2=0.99$
Animal G	$Y=1.03x-20.2$; $r^2=0.93$	$Y=1.00x+10.3$; $r^2=0.99$
Animal P	$Y=0.95x+3.5$; $r^2=0.99$	$Y=1.02x-10.6$; $r^2=0.97$
All animals	$Y=1.02x-5.2$; $r^2=0.92$	$Y=1.09x+9.0$; $r^2=0.92$

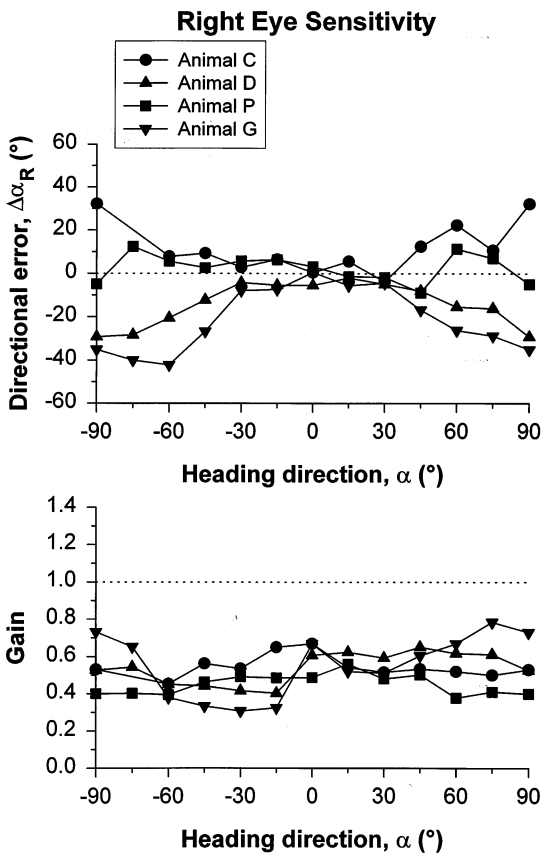

Fig. 3. Dependence of fitted parameters of the right eye on heading direction. For each animal, the directional errors ($\Delta\alpha_R$) and gains (k_R) were estimated by fitting Eqs. (A5a) and (A5b) to responses for each heading direction.

3.3. Version and vergence responses

In a system that produces largely disjunctive movements, an alternative way to decompose binocular movements is version and vergence (rather than right and left eye responses). The simplified Eqs. (A8) and (A9) have been used to quantify the dependence of version and vergence on gaze and heading directions. As shown in Fig. 5, version sensitivity exhibited the hypothesized dependence on eye position for all heading directions. In fact, the individual (thick lines) and the global fits (thin lines) were closely aligned for all heading directions. Indeed, the directional error, $\Delta\alpha$, estimated when fitting Eq. (A9) to data for each heading direction was small ($<20°$) for all but animal C (circles in Fig. 6, top). Similarly to the results obtained when examining the sensitivities of each eye separately, the directional errors characterizing the direction dependence of version sensitivity, $\Delta\alpha_s$, exhibited a significant dependence on heading, but not on gaze direction (Table 3). The gain of the version response was consistently small, averaging ~ 0.5 independently of heading direction (Fig. 6, bottom; for statistical comparisons, see Table 3).

Vergence sensitivity behaved in several respects differently from the conjugate component of the response (Fig. 7). When Eq. (A8) was fitted separately to each movement direction, fits were good with small mean-square-error values, however, directional errors, $\Delta\alpha_e$, were larger than those of version (Fig. 8, top) and independent of movement direction (Table 3). The global fits, where all data were fitted simultaneously, also yielded large directional errors (Table 1; see also thin lines in Fig. 8). Since Eq. (A8) fitted to the vergence sensitivity data was derived on the assumption that $k_R = k_L$ and $\Delta\alpha_R = \Delta\alpha_L$, it is possible that the large directional errors of vergence sensitivity were due to the small differences in these values between the right and left eyes. However, there was no correlation between the vergence errors $\Delta\alpha_e$ and either one of the following measures: $|\Delta\alpha_R - \Delta\alpha_L|$ and $|k_R/k_L - 1|$ ($R^2 \ll 0.10$).

Despite largely undercompensatory version gains, vergence gains were large (Fig. 8, bottom). For fore–aft motion directions ($\alpha = 0°$), gains were near unity in all but one animal (the same animal who exhibited small

Table 3
Dependence of fitted parameters ($\Delta\alpha$ and k) on heading and gaze direction[a]

	Right eye	Left eye	Version	Vergence
Tuning versus heading direction				
$\Delta\alpha$	$F(6,19) = 15.8^{c}$	$F(6,19) = 3.4^{b}$	$F(6,19) = 7.1^{c}$	$F(5,10) = 1.7$
k	$F(6,19) = 0.94$	$F(6,19) = 0.25$	$F(6,19) = 2.9^{b}$	$F(5,10) = 8.4^{c}$
Tuning versus gaze direction				
$\Delta\alpha$	$F(2,7) = 2.0$	$F(2,7) = 0.07$	$F(2,7) = 0.64$	$F(2,7) = 0.96$
k	$F(2,7) = 1.5$	$F(2,7) = 0.87$	$F(2,7) = 1.6$	$F(2,7) = 0.43$

[a] Statistical comparisons are based on analysis of variance. If no superscript is provided, the respective dependence was not statistically significant. Data from four animals (right eye, left eye and version) or three animals (for vergence), animal P was not included because of unsatisfactory fits for several heading directions; see Section 2).
[b] Significance at 0.05 level.
[c] Significance at 0.01 level.

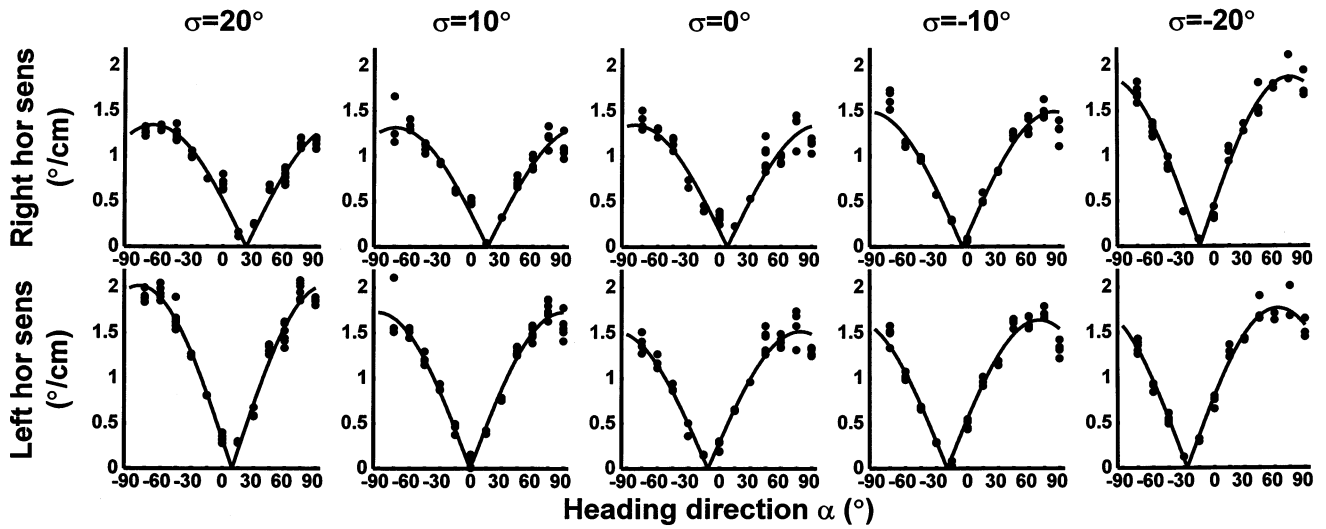

Fig. 4. Tuning of the horizontal sensitivity of the right and left eyes as a function of heading direction for five different eye positions (σ). The superimposed lines are fits of Eqs. (A5a) and (A5b) to data for each eye position separately.

gains also in McHenry & Angelaki, 2000). For in-between orientations, gains tended to be larger than unity. This dependence of vergence gain on movement direction was statistically significant (Table 3).

4. Discussion

The influence of gaze and heading directions on vestibularly-driven binocular eye movements was examined here during rapid linear head oscillations. We show that the translational VOR is compatible with a gaze-stabilization hypothesis that predicts a characteristic dependence of vestibularly-induced eye velocity on gaze and heading directions. A detailed analysis of the nature of the predicted gaze- and heading direction dependencies reveals characteristic differences for the conjugate (version) and disjunctive (vergence) part of the translational VOR. This distinction might be functionally important, since the thresholds for monocular and binocular visual acuity are different (Brown, 1972; Steinman, Haddad, Skavenski, & Wyman, 1973; Steinman, Cushman, & Martins, 1982; Sarmiento, 1975; Westheimer & McKee, 1975; Murphy, 1978). We suggest that the translational VOR is optimized for stabilizing the relative orientation of the gaze lines, a property which is of paramount importance to enable and maintain stereovision.

4.1. Gaze line stabilization hypothesis

In any given heading direction, vestibular signals from the otolith organs of the inner ear encode the direction of the movement and transmit that information to the brainstem, including the motoneurons innervating the eye muscles. This information is used to generate reflexive eye movements that aim to reduce retinal image slip and provide stable processing of the visual surround. Because retinal image slip cannot be generally avoided during translation, the otolith signals

can at most generate eye movements that optimize locally the visual acuity. Although it is natural to assume that the trVOR stabilizes images on the fovea (Paige & Tomko, 1991b; Tomko & Paige, 1992), the implications of this hypothesis have so far not been studied. This work shows that the movements of both eyes can be modeled on the basis of the geometrical constraints dictated by the requirement to control binocular gaze direction in space (binocular gaze stabilization hypothesis). We find that the gains of each eye are generally small (~ 0.5) during near target viewing and that there is a significant bias in the spatial tuning of these eye movements as a function of heading direction. Whereas they are most accurately tuned for headings $\pm 30°$ from the fore–aft axis, tuning deteriorates for movements close to the lateral axis.

Part of the systematic and significant dependence of directional errors on heading direction could be explained by the sinusoidal dependence of ocular sensitivity on the direction of heading. During fore–aft motion, for example, Eqs. (A5a) and (A5b) operate within the linear range of the sine function. During lateral motion, on the other hand, the sine function depends very little on changes in heading and gaze directions (the argument of the sine function in the numerator of Eqs. (A5a) and (A5b) is close to 90°). To illustrate this effect, we computed the confidence intervals on the estimated parameter, α, based on the assumption that the experimental errors in the response derive from a normal distribution (see Appendix A). The simulation shows that the confidence interval increases significantly for headings away from the fore–aft axis (Fig. 10). This suggests that the deviation from ideal behavior could be due to the particular geometrical bias that is inherent in fitting the nonlinear model to experimental data. Therefore, the larger errors in heading directions close to 90° may not necessarily imply a less accurate coding of lateral heading directions. A comparison between the experimental data and model simulations rather suggests that the vestibulo-ocular responses closely exhibit the expected geometrical dependencies, not only in terms of mean sensitivity, but also in terms of the expected statistical variability of responses.

The clearest deviation from the expected geometrical behavior is the largely undercompensatory gains for either eye and the version (conjugate) responses. Similar undercompensatory gains have been reported during

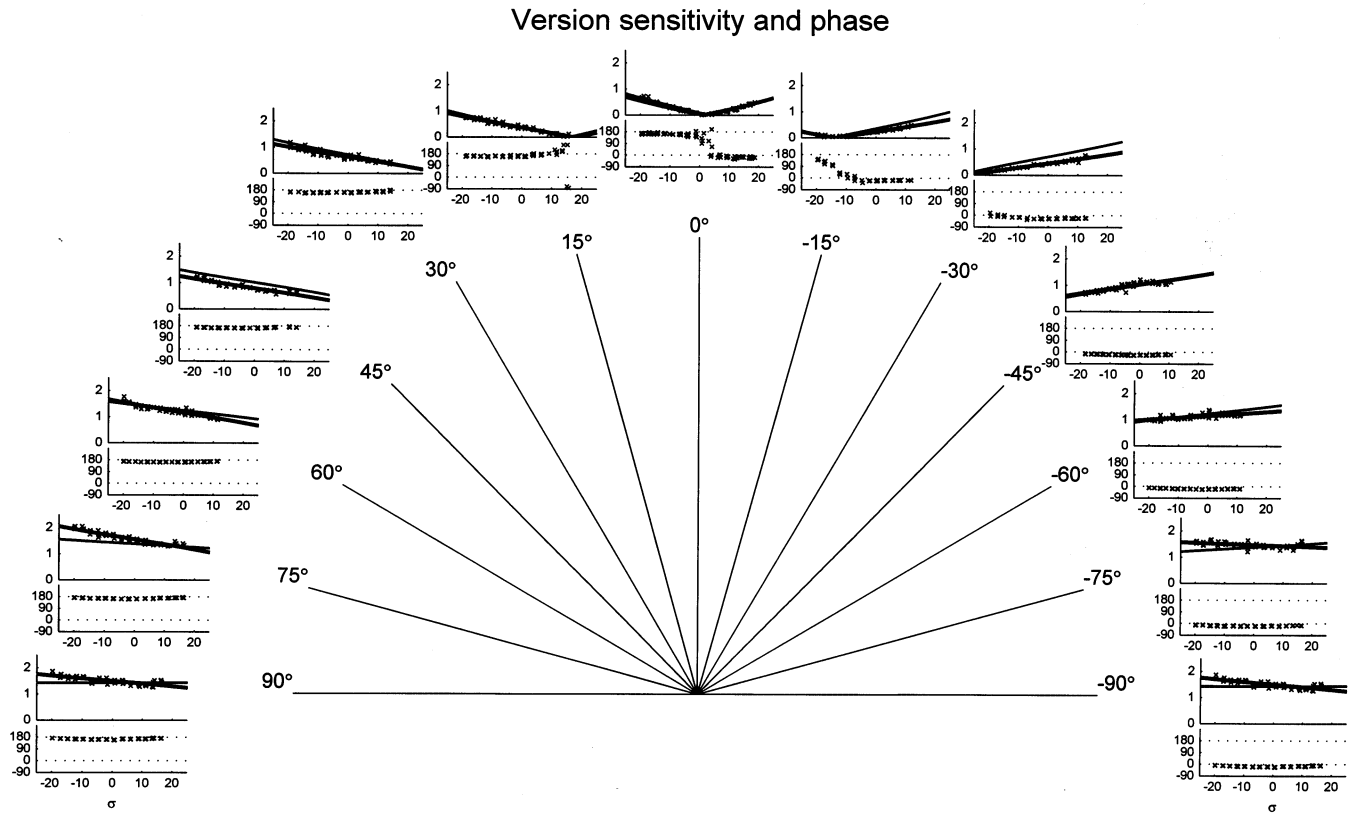

Fig. 5. Tuning of the horizontal version sensitivity as a function of version (σ). Response sensitivity (°/cm) and phase (°) are both plotted for each movement direction. The superimposed thin lines are fits of Eq. (A9) to the whole data set (i.e. all heading directions simultaneously; parameters are included in Table 1). The superimposed thick lines are fits of Eq. (A9) to each heading direction separately. An orientation of $\alpha = 0°$ corresponds to fore–aft motion, whereas orientations of $\alpha = \pm 90°$ correspond to lateral motion stimuli.

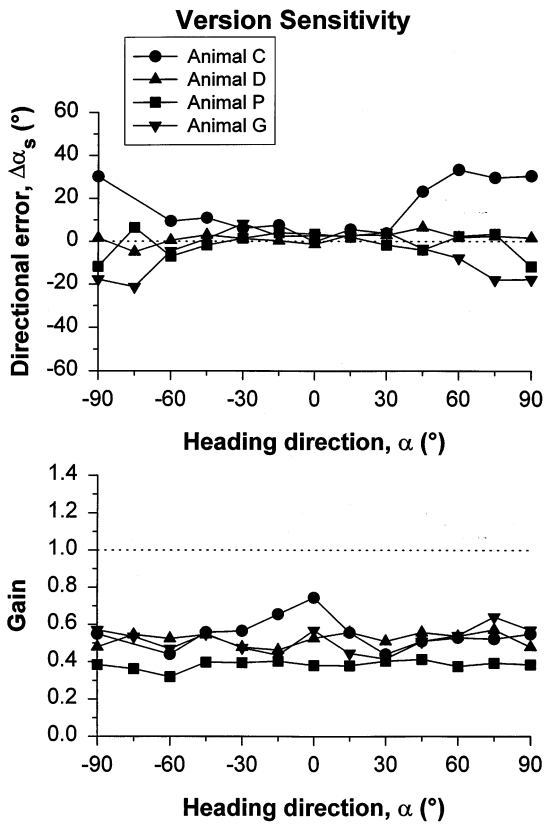

Fig. 6. Tuning of version sensitivity as a function of heading direction. For each animal, the directional errors ($\Delta\alpha_s$) and gains (k_s) were estimated by fitting Eq. (A9) to responses for each heading direction.

near target viewing in all previous studies of the trVOR (Paige & Tomko, 1991a; Paige & Tomko, 1991b; Schwarz & Miles, 1991; Telford et al., 1997; Angelaki et al., 2000a; Angelaki et al., 2000b; McHenry & Angelaki, 2000). Even though trVOR sensitivity has been shown to be a function of both vergence angle and accommodation (Paige & Tomko, 1991a; Paige & Tomko, 1991b; Schwarz & Miles, 1991), other measures might also be relevant. For example, the perception of depth and viewing distance depends on numerous other factors, including horizontal and vertical disparities, size cues and motion parallax (e.g. Howard, 1995). The reason behind the low gains could be the fact that all trVOR data so far have been recorded either in darkness or in the presence of a single small target. Under these conditions, the central coding of target distance (related to 'ε', in Eqs. (A2)–(A9) could be underestimated.

The fact that the vestibularly-driven eye movements during translation are functionally related to the need to stabilize the fovea (rather than the peripheral vision) would suggest that the translational VOR should be considered as a gaze stabilization system similarly, for example, to smooth pursuit eye movements. That is, its functional goal is to stabilize the gaze lines, without any obvious regard for peripheral vision. This conclusion is further supported by the fact that eye velocity during lateral translation might exhibit the appropriate 3-D characteristics that could be consistent with Listing's law (Angelaki et al., 2000a). In this regard, the translational VOR seems to differ from the rotational VOR, where it has been demonstrated that primate vestibularly-driven eye movements during head rotation attempt to stabilize images not only on the fovea, but also on the entire retina (Misslisch & Hess, 2000).

Very little is currently known about the neural substrates that generate these responses. It will be a challenge for future work to understand the neural processing that converts otolith afferent signals, coding merely heading direction, into this elaborate repertoire of eye movements that are highly tuned to the underlying geometry for binocular gaze stabilization. It should, however, be pointed out that the gaze stabilization model examined here considers only how the system controls the lines of sight, i.e. the horizontal and vertical coordinates of the two eyes as they maintain fixation on the target. The model does not care about the relative torsional orientation of the two eyes which determine cyclodisparity, a rather important parameter in near vision and stereovision.

4.2. Vergence eye movements and stereopsis

When the difference in the movement of the two eyes was evaluated according to the geometrical model, vergence exhibited high gains (unity or higher than unity) but in general larger directional errors. Higher vergence than version gains were also reported in a more extensive investigation of binocular eye movements at different viewing distances during fore–aft motion (McHenry & Angelaki, 2000). In fact, the large vergence gains, in the presence of strongly undercompensatory left and right eye sensitivities, were shown to be elicited because of asymmetries in the adduction/abduction responses and opposite shifts of the zero sensitivity gaze directions for the left and right eyes (McHenry & Angelaki, 2000). The present results show that high vergence gains are also present for oblique heading directions.

The consistent trend for nearly unity vergence gains for headings close to the fore–aft direction might be functionally important to maintain binocular gaze in the same depth plane regardless of an inappropriate version velocity gain. During the small (5.1 cm/s peak) oscillations used here, the horizontal modulation in eye position (velocity) would be maximally $\sim 0.2°$ ($\sim 14°$/s). Thus version gains of ~ 0.5 would result in image slip with a peak of $\sim 0.1°$ ($\sim 7°$/s). These values are approximately double those reported for maintaining a good visual acuity (Brown, 1972; Steinman et al., 1973, 1982; Westheimer & McKee, 1975; Murphy, 1978; De-

mer & Amjadi, 1993; Demer, Honrubia, & Baloh, 1994). The peak modulation in vergence position/velocity predicted by Eqs. (A1)–(A9) is $\sim 0.035°$ ($\sim 2.2°/s$). The high gain of vergence responses could be related to the very low threshold for stereovision, which is in the order of seconds of arc for foveal vision (Sarmiento, 1975). The present results, as well as those of McHenry & Angelaki (2000), suggest that vestibularly driven eye movements help to minimize head movement-induced modulation of the fixation plane, at least for heading directions near fore–aft. Such a vestibularly-driven stabilization of the fixation plane operates at frequencies higher than those of disparity-driven vergence eye movements and could be important for the maintenance of stereovision, even when the velocity gain of the version movement is low.

Acknowledgements

Supported by grants from NIH (EY12814, EY10851 and DC04160). The authors are thankful to Q. McHenry, A. Haque and B. Harris for technical assistance.

Appendix A

A.1. Equations describing eye movement sensitivity based on the gaze stabilization hypothesis

Consider the vectors $\underline{r} = (r_x\ r_y\ r_z)^T$ and $\underline{l} = (l_x\ l_y\ l_z)^T$, which point from the center of the right and the left eye to the target of interest in space (Fig. 9). The lengths of these vectors, denoted by $\|\underline{r}\| = \sqrt{r_x^2 + r_y^2 + r_z^2}$ and $\|\underline{l}\| = \sqrt{l_x^2 + l_y^2 + l_z^2}$, are a measure of the viewing distance between the respective eye and the target. The horizontal position of each eye is related to these vectors by the inverse tangent as $\theta_R = \tan^{-1}(r_y/r_x)$ and $\theta_L = \tan^{-1}(l_y/l_x)$. From these angles we compute the vergence angle as $\varepsilon = \theta_R - \theta_L$ and the version angle as $\sigma = (\theta_R + \theta_L)/2$. Furthermore, we can also express the horizontal eye velocity as a function of the x- and y-components of the moving gaze vector $r(t)$ by computing the time derivative as follows:

$$\dot{\theta}_R = \frac{d}{dt}\left(\tan^{-1}\frac{r_y}{r_x}\right) = \frac{\dot{r}_y r_x - \dot{r}_x r_y}{r_x^2 + r_y^2} = \frac{\sqrt{\dot{r}_x^2 + \dot{r}_y^2}}{\sqrt{r_x^2 + r_y^2}}\left(\frac{\dot{r}_y}{\sqrt{\dot{r}_x^2 + \dot{r}_y^2}}\frac{r_x}{\sqrt{r_x^2 + r_y^2}} - \frac{\dot{r}_x}{\sqrt{\dot{r}_x^2 + \dot{r}_y^2}}\frac{r_y}{\sqrt{r_x^2 + r_y^2}}\right) \quad \text{(A1)}$$

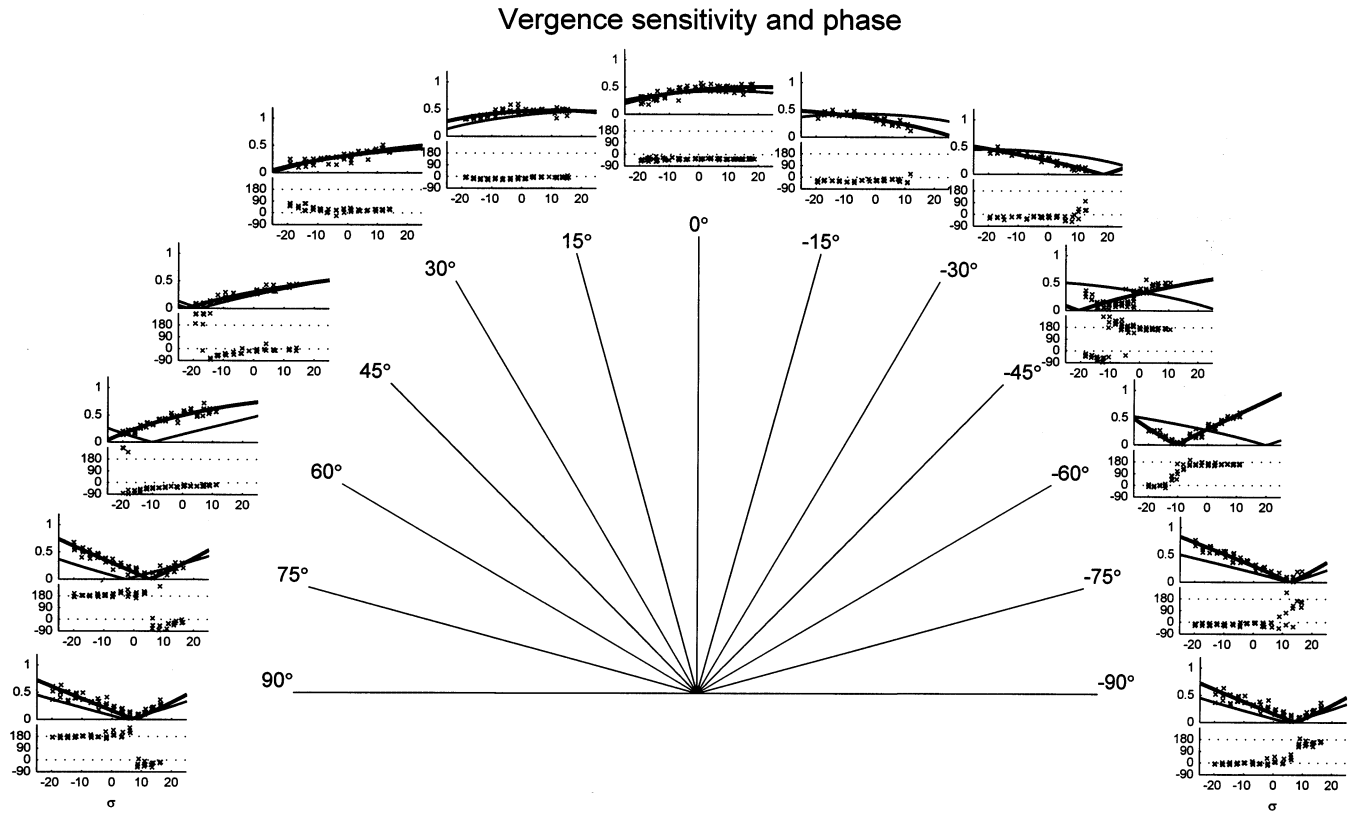

Fig. 7. Tuning of the horizontal vergence sensitivity as a function of version eye position (σ). Response sensitivity (°/cm) and phase (°) are both plotted for each movement direction. The superimposed thin lines are fits of Eq. (A8) to the whole data set (i.e. all heading directions simultaneously; parameters are included in Table 1). The superimposed thick lines are fits of Eq. (A8) to each heading direction separately. An orientation of $\alpha = 0°$ corresponds to fore–aft motion, whereas orientations of $\alpha = \pm 90°$ correspond to lateral motion stimuli.

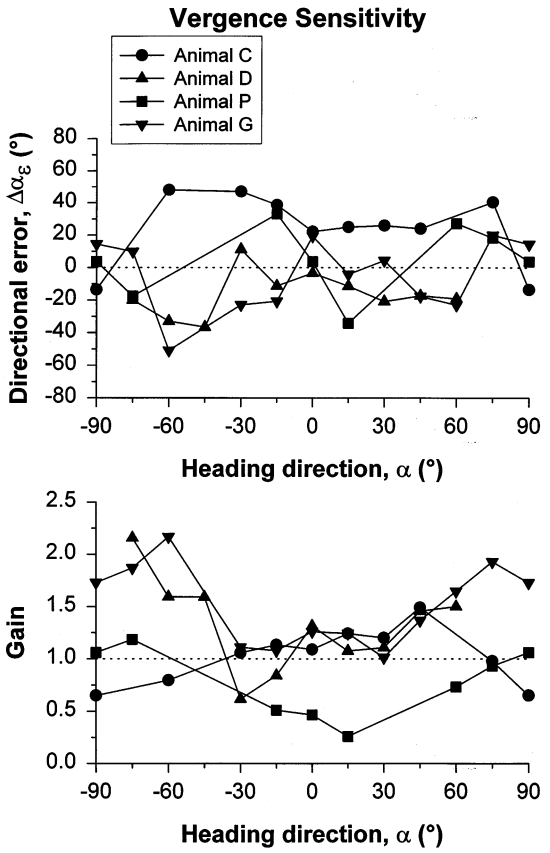

Fig. 8. Tuning of vergence sensitivity as a function of heading direction. For each animal, the directional errors ($\Delta\alpha_\varepsilon$) and gains (k_ε) were estimated by fitting Eq. (A8) to data for each heading direction.

By introducing the viewing distance, $d_R = \sqrt{r_x^2 + r_y^2}$, as well as the magnitude and the direction of the gaze velocity vector in the horizontal plane, $v_R = \sqrt{\dot{r}_x^2 + \dot{r}_y^2}$

$$\alpha_R = \tan^{-1}\left(\frac{\dot{r}_y}{\dot{r}_x}\right) = \sin^{-1}\left(\frac{\dot{r}_y}{\sqrt{\dot{r}_x^2 + \dot{r}_y^2}}\right) = \cos^{-1}\left(\frac{\dot{r}_x}{\sqrt{\dot{r}_x^2 + \dot{r}_y^2}}\right)$$

(Fig. 9), the second line of Eq. (A1) can be expressed as:

$$\dot{\theta}_R = \frac{v_R}{d_R}\sin(\alpha_R - \theta_R) \tag{A2}$$

An analogous relation holds for the left eye. In the following step, we express the viewing distance, d_R, in the horizontal plane for the right eye as a function of the inter-ocular distance, d_{ioc}, the vergence angle, ε, and right eye position, θ_R, as follows:

$$d_R = d_{ioc}\left(\sin\theta_R + \frac{\cos\theta_R}{\tan\varepsilon}\right) = d_{ioc}\frac{\cos(\varepsilon - \theta_R)}{\sin\varepsilon} \tag{A3a}$$

and similar for the left eye:

$$d_L = d_{ioc}\left(\frac{\cos\theta_L}{\tan\varepsilon} - \sin\theta_L\right) = d_{ioc}\frac{\cos(\theta_L + \varepsilon)}{\sin\varepsilon} \tag{A3b}$$

Finally, we obtain the horizontal eye velocity as a function of the horizontal gaze angle, the magnitude and direction of gaze velocity and the vergence angle by combining Eqs. (A2), (A3a) and (A3b):

$$\dot{\theta}_R = v_R\frac{\sin\varepsilon}{d_{ioc}}\frac{\sin(\alpha_R - \theta_R)}{\cos(\theta_R - \varepsilon)} \tag{A4a}$$

$$\dot{\theta}_L = v_L\frac{\sin\varepsilon}{d_{ioc}}\frac{\sin(\alpha_L - \theta_L)}{\cos(\theta_L + \varepsilon)} \tag{A4b}$$

For binocular tracking of a moving target, the speed of the two gaze vectors must be equal and opposite to target velocity. If we assume that the tracking gain is less than unity we can state that $v_R = k_R v_{target}$ and $v_L = k_L v_{target}$ where k_R, k_L are the gains of the angular speed of the right and left gaze vectors. Thus, the response sensitivities of the right and left eyes during tracking of a near target can be expresses as follows:

$$\frac{\dot{\theta}_R}{v_{target}} = k_R\frac{\sin\varepsilon}{d_{ioc}}\frac{\sin(\alpha + \Delta\alpha_R - \theta_R)}{\cos(\theta_R - \varepsilon)} \tag{A5a}$$

$$\frac{\dot{\theta}_L}{v_{target}} = k_L\frac{\sin\varepsilon}{d_{ioc}}\frac{\sin(\alpha + \Delta\alpha_L - \theta_L)}{\cos(\theta_L + \varepsilon)} \tag{A5b}$$

where v_{target} and α describe the speed and direction of target motion and $\Delta\alpha_R$, $\Delta\alpha_L$ are the directional errors between the gaze and target velocity of the right and left eye (i.e. $\alpha_R = \alpha + \Delta\alpha_R$, $\alpha_L = \alpha + \Delta\alpha_L$). For perfect

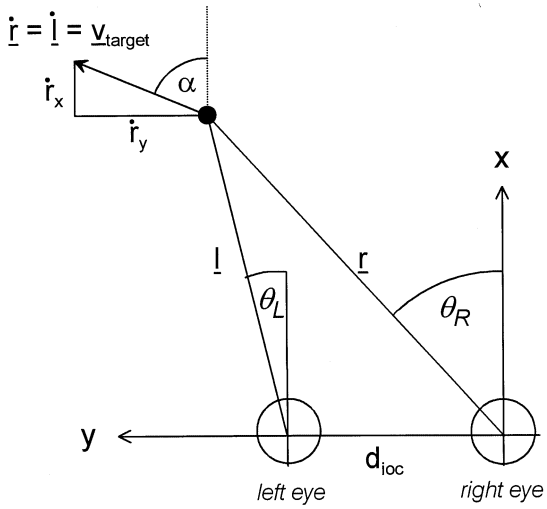

Fig. 9. Schematic diagram describing the geometrical relationships of the gaze-stabilization hypothesis for an arbitrary heading and gaze direction. The associated movement of the subject corresponds to an equivalent target motion with velocity v_{target} along a heading direction defined by angle α. The target position is defined by the intersection of the two gaze lines, with θ_R and θ_L being the horizontal Fick angles of the right and left eye, respectively. The interocular distance is d_{ioc}, whereas r is the center of rotation to target distance of the right eye and l is the center of rotation to target distance of the left eye.

binocular tracking of a target, the velocity of each gaze line must match the magnitude and direction of target velocity (i.e. $k_R = k_L = 1$, and $\alpha_R = \alpha_L = \alpha$). The same equations also describe the movement of the gaze lines during fixation of a target while the head moves. In this case, the target moves relative to the head with a velocity that is equal and opposite to head velocity.

Since the sensitivities are in general different for each eye, binocular eye movements can be decomposed into conjugate (version) and disjunctive (vergence) components. Accordingly, the dynamic vergence and version sensitivities are:

$$\frac{\dot{\varepsilon}}{v_{target}} = \frac{\sin\varepsilon}{d_{ioc}}\left(k_R\frac{\sin(\alpha+\Delta\alpha_R-\theta_R)}{\cos(\theta_R-\varepsilon)} - k_L\frac{\sin(\alpha+\Delta\alpha_L-\theta_L)}{\cos(\theta_L+\varepsilon)}\right) \quad (A6)$$

$$\frac{\dot{\sigma}}{v_{target}} = -\frac{\sin\varepsilon}{2d_{ioc}}\left(k_R\frac{\sin(\alpha+\Delta\alpha_R-\theta_R)}{\cos(\theta_R-\varepsilon)} + k_L\frac{\sin(\alpha+\Delta\alpha_L-\theta_L)}{\cos(\theta_L+\varepsilon)}\right) \quad (A7)$$

where $\dot{\varepsilon} = \dot{\theta}_R - \dot{\theta}_L$, $\dot{\sigma} = (\dot{\theta}_R + \dot{\theta}_L)/2$, k_R,k_L represent the gains of the speed of the right and left eye gaze vectors and $\Delta\alpha_R$, $\Delta\alpha_L$ are the directional errors between gaze and target velocity of the right and left eye (see above).

If the gains and directional errors of the right and left eye are similar (i.e. $k_R \cong k_L$ and $\Delta\alpha_R \cong \Delta\alpha_L$), Eqs. (A6) and (A7) can be further simplified to:

$$\frac{\dot{\varepsilon}}{v_{target}} = -k_\varepsilon\frac{\sin^2\varepsilon}{d_{ioc}}\frac{\cos(\alpha+\Delta\alpha_\varepsilon-\theta_R-\theta_L)}{\cos\theta_R\cos\theta_L} = -k_\varepsilon\frac{\sin^2\varepsilon}{d_{ioc}}\frac{\cos(\alpha+\Delta\alpha_\varepsilon-2\sigma)}{\cos(\sigma+\varepsilon/2)\cos(\sigma-\varepsilon/2)} \quad (A8)$$

$$\frac{\dot{\sigma}}{v_{target}} = k_s\frac{\sin\varepsilon}{2d_{ioc}}\frac{\sin(\alpha+\Delta\alpha_s)+\cos\varepsilon\sin(\alpha+\Delta\alpha_s-\theta_R-\theta_L)}{\cos\theta_R\cos\theta_L} = k_s\frac{\sin\varepsilon}{2d_{ioc}}\frac{\sin(\alpha+\Delta\alpha_s)+\cos\varepsilon\sin(\alpha+\Delta\alpha_s-2\sigma)}{\cos(\sigma+\varepsilon/2)\cos(\sigma-\varepsilon/2)} \quad (A9)$$

A.2. Confidence limits on estimated gain and directional parameters as a function of gaze and heading directions

When fitting the non-linear geometrical model to actual experimental data, a statistical bias in the least squares estimation is expected, for example, based on the discrepancy between the relatively small range of gaze angles tested and the wide range of heading directions. In applying Eq. (A2) and its corollaries (Eqs. (A5a), (A5b), (A8) and (A9)) to experimental data it would be important to obtain an estimate of the inherent statistical bias of the least squares fitted parameters. The statistical characteristics of the fitted parameters can be obtained by minimizing the χ^2 merit function of the non-linear least squares fit of Eq. (A2) (Press, Teukolsky, Vetterling, & Flannery, 1992):

$$\chi^2(k,\alpha) = \sum_{i=1}^{N}\left[\frac{\dot{\theta}^i_R - k\sin(\alpha-\theta^i_R)/\cos(\theta^i_R-\varepsilon)}{\varsigma_i}\right]^2 \quad (A10)$$

where ς is the S.D. of the measured (mean) eye velocities $\dot{\theta}^i_R$ for each gaze direction θ^i_R (N = total number of gaze directions tested). Assuming that the measurement errors in eye velocity are normally distributed (Gaussian noise), the confidence limits on the estimated model parameters can be computed directly from the Hessian matrix of the χ^2 merit function (with $a_1 = k$ and $a_2 = \alpha$):

$$\frac{\partial\chi^2}{\partial a_n\partial a_m} = \sum_{i=1}^{N}\frac{1}{\varsigma_i^2}\left[\frac{\partial\dot{\theta}_R}{\partial a_n}\frac{\partial\dot{\theta}_R}{\partial a_m} - [\dot{\theta}^i_R - \dot{\theta}_R]\frac{\partial^2\dot{\theta}_R}{\partial a_m\partial a_m}\right] \approx \sum_{i=1}^{N}\frac{1}{\varsigma_i^2}\frac{\partial\dot{\theta}_R}{\partial a_n}\frac{\partial\dot{\theta}_R}{\partial a_m} \quad (n,m=1,2) \quad (A11)$$

At the minimum of a successful least squares fit, the term $[\dot{\theta}^i_R - \dot{\theta}_R]$ in Eq. (A11) varies randomly around zero. Thus, only the first term which depends on the first partial derivatives of the model $\dot{\theta}_R = \dot{\theta}_R(\theta^i_R, k, \alpha)$ (see Eqs. (A5a) and (A5b)) with respect to the parameters k and α have to be considered (right-hand side of Eq. (A11)). The statistical errors δk and $\delta\alpha$ of the model parameters can now be obtained from the inverse of one-half of the Hessian matrix as follows (Press et al., 1992):

$$\delta k = \pm 2\sqrt{C_{11}} \quad (A12)$$

$$\delta\alpha = \pm 2\sqrt{C_{22}} \quad (A13)$$

where $C_{ik} = \frac{1}{2}\left[\frac{\partial^2\chi^2}{\partial a_i\partial a_k}\right]^{-1}$ is the covariance matrix of the non-linear least squares problem.

An evaluation of Eqs. (A12) and (A13) using a S.D. of $\varsigma = 0.29°$/cm (10% of peak sensitivity; assumed to be constant for all gaze and heading directions) is illustrated in Fig. 10. The 95% confidence limits on δk vary between about ± 5 to ± 20% (relative to unity gain; red solid lines in Fig. 10, bottom). The confidence limits on $\delta\alpha$ are less than $\pm 7°$ for heading directions between $\pm 30°$ and larger than $\pm 10°$ for heading directions exceeding 60° ($P = 0.05$; red solid lines in Fig. 10, top). For better comparison with the experimental data, we based these simulations on 17 equally spaced fixations between $\pm 20°$ relative to straight-ahead and a mean vergence angle of 8.6°. The simulations also show that

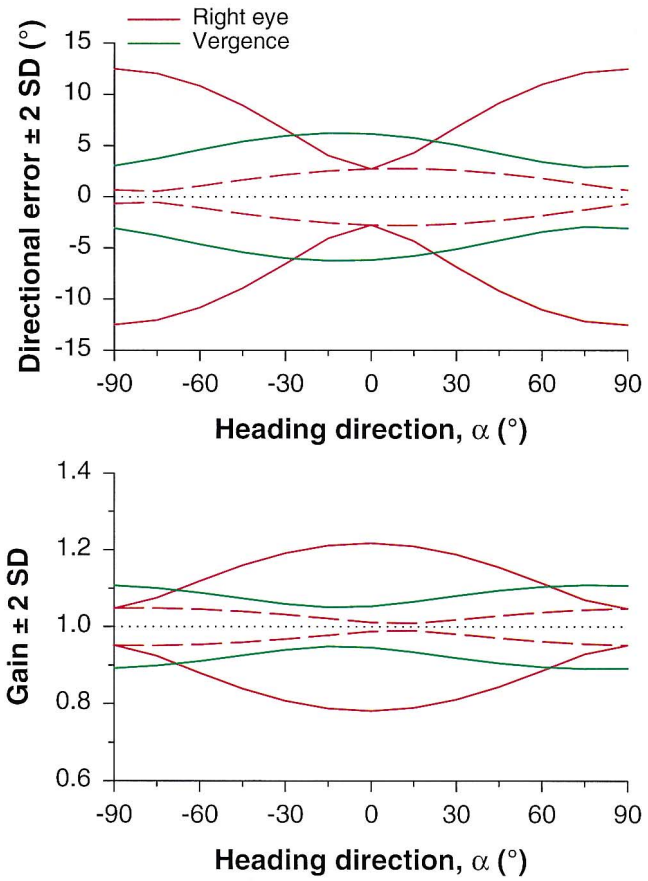

Fig. 10. Confidence limits for the fitted parameters as a function of heading direction. The curves show simulations of the 95% confidence limits (2 S.D., $P = 0.05$) of the estimated directional error (top) and gain (bottom) of the right eye (red) and vergence (green). Simulations are based on 17 equally spaced fixations in the interval $\pm 20°$ (solid lines) and in the interval $\pm 90°$ (dashed lines), centered around zero (straight ahead). Simulation parameters: $\varsigma = 0.29°/\text{cm}$, $\varepsilon = 8.6°$ and $d_{\text{ioc}} = 3$ cm.

the confidence intervals depend on the angular range of fixations tested. For example, if one could include fixations over an interval as large as $\pm 90°$ the confidence limits would not only be significantly reduced (for the same number of fixations) but also less dependent on heading direction (see dashed red curves in Fig. 10). The least squares fit of vergence responses shows the reverse dependence of confidence limits on heading direction compared to the responses from each eye (Fig. 10, compare green with red lines).

References

Angelaki, D. E. (1998). Three-dimensional organization of otolith-ocular reflexes in rhesus monkeys. III. Responses to translation. *Journal of Neurophysiology*, *80*, 680–695.

Angelaki, D. E., & McHenry, M. Q. (1999). Short-latency primate vestibulo-ocular responses during translation. *Journal of Neurophysiology*, *82*, 1651–1654.

Angelaki, D. E., McHenry, M. Q., & Hess, B. J. M. (2000a). Primate translational vestibulo-ocular reflexes. I. High frequency dynamics and three-dimensional properties during lateral motion. *Journal of Neurophysiology*, *83*, 1637–1647.

Angelaki, D. E., McHenry, M. Q., Dickman, J. D., & Perachio, A. A. (2000b). Primate translational vestibulo-ocular reflexes. III. Effect of bilateral labyrinthine electrical stimulation. *Journal of Neurophysiology*, *83*, 1662–1676.

Brown, B. (1972). Resolution thresholds for moving targets at the fovea and in the peripheral retina. *Vision Research*, *12*, 293–304.

Busettini, C., Miles, F. A., & Schwarz, U. (1991). Ocular responses to translation and their dependence on viewing distance: II. Motion of the scene. *Journal of Neurophysiology*, *66*, 865–878.

Busettini, C., Miles, F. A., Schwarz, U., & Carl, J. R. (1994). Human ocular responses to translation of the observer and of the scene: dependence on viewing distance. *Experimental Brain Research*, *100*, 484–494.

Busettini, C., Masson, G. S., & Miles, F. A. (1996a). A role for stereoscopic depth cues in the rapid visual stabilization of the eyes. *Nature*, *380*, 342–345.

Busettini, C., Miles, F. A., & Krauzlis, R. J. (1996b). Short-latency disparity vergence responses and their dependence on a prior saccadic eye movement. *Journal of Neurophysiology*, *75*, 1392–1410.

Busettini, C., Masson, G. S., & Miles, F. A. (1997). Radial optic flow induces vergence eye movements with ultra-short latencies. *Nature*, *390*, 512–515.

Bush, G. A., & Miles, F. A. (1996). Short-latency compensatory eye movements associated with a brief period of free fall. *Experimental Brain Research*, *108*, 337–340.

Demer, J. L., & Amjadi, F. (1993). Dynamic visual acuity of normal subjects during vertical optotype and head motion. *Investigative Ophthalmology and Visual Science*, *34*, 1894–1906.

Demer, J. L., Honrubia, V., & Baloh, R. W. (1994). Dynamic visual acuity: A test for oscillopsia and vestibulo-ocular reflex function. *American Journal of Otology*, *15*, 340–347.

Haustein, W. (1989). Considerations on Listing's law and primary position by means of a matrix description of eye position control. *Biological Cybernetics*, *60*, 411–420.

Howard, I. P. (1995). *Binocular vision and stereopsis*. New York: Oxford University Press.

Masson, G. S., Busettini, C., & Miles, F. A. (1997). Vergence eye movements in response to binocular disparity without the perception of depth. *Nature*, *389*, 283–286.

McHenry, M. Q., & Angelaki, D. E. (2000). Primate translational vestibulo-ocular reflexes. II. Vergence and version responses during fore–aft motion. *Journal of Neurophysiology*, *83*, 1648–1661.

Miles, F. A. (1998). The neural processing of 3-D visual information: evidence from eye movements. *European Journal of Neuroscience*, *10*, 811–822.

Miles, F. A., Schwarz, U., & Busettini, C. (1991). The parsing of optic flow by the primate oculomotor system. In A. Gorea, *Representations of vision*: *trends and tacit assumptions in vision research* (pp. 185–199). Cambridge: Cambridge University Press.

Misslisch, H., & Hess, B. J. M. (2000). Three-dimensional vestibulo-ocular reflex of the monkey: optimal retinal image stabilization versus Listing's law. *Journal of Neurophysiology*, *83*, 3264–3276.

Murphy, B. J. (1978). Pattern thresholds for moving and stationary gratings during smooth eye movement. *Vision Research*, *18*, 521–530.

Paige, G. D., & Tomko, D. L. (1991a). Eye movements responses to linear head motion in the squirrel monkey I. Basic characteristics. *Journal of Neurophysiology*, *65*, 1170–1182.

Paige, G. D., & Tomko, D. L. (1991b). Eye movement responses to linear head motion in the squirrel monkey II. Visual–vestibular interactions and kinematic considerations. *Journal of Neurophysiology*, *65*, 1183–1196.

Press, W. H., Teukolsky, S. A., Vetterling, W. T., & Flannery, B. P. (1992). *Numerical recipes in C*. Cambridge: Cambridge University Press.

Sarmiento, R. F. (1975). The stereoacuity of macaque monkey. *Vision Research*, *15*, 493–498.

Schwarz, U., & Miles, F. A. (1991). Ocular responses to translation and their dependence on viewing distance: I. Motion of the observer. *Journal of Neurophysiology*, *66*, 851–864.

Schwarz, U., Busettini, C., & Miles, F. A. (1989). Ocular responses to translation are inversely proportional to viewing distance. *Science*, *245*, 1394–1396.

Steinman, R. M., Haddad, G. M., Skavenski, A. A., & Wyman, D. (1973). Miniature eye movements. *Science*, *181*, 810–819.

Steinman, R. M., Cushman, W. B., & Martins, A. J. (1982). The precision of gaze. *Human Neurobiology*, *1*, 97–109.

Telford, L., Seidman, S. H., & Paige, G. D. (1997). Dynamics of squirrel monkey linear vestibuloocular reflex and interactions with fixation distance. *Journal of Neurophysiology*, *78*, 1775–1790.

Tomko, D. L., & Paige, G. D. (1992). Linear vestibuloocular reflex during motion along axes between nasooccipital and interaural. *Annals of the New York Academy of Science*, *656*, 233–241.

Westheimer, G., & McKee, S. P. (1975). Visual acuity in the presence of retinal image motion. *Journal of the Optical Society of America*, *65*, 847–850.